Environmental Microbiology (in review)

Structural and functional skin microbiota on cane toads across 16,000 km of invaded range

Running title: Toad skin microbes across invaded range

Chava L. Weitzman*[1], chava.weitzman2@cdu.edu.au, ORCId - 0000-0002-6103-1885

Kimberley Day[1], k.day@aims.gov.au

Gregory P. Brown[2], greg.brown@mq.edu.au, ORCId - 0000-0002-2924-9040

Karen Gibb[1], karen.gibb@cdu.edu.au, ORCId - 0000-0003-2987-883X

Keith Christian[1], keith.christian@cdu.edu.au, ORCId - 0000-0001-6135-1670

[1] Research Institute for the Environment and Livelihoods, Charles Darwin University, Darwin, NT, 0909, Australia

[2] Department of Biological Sciences, Macquarie University, New South Wales, 2109, Australia

*Corresponding author: chava.weitzman2@cdu.edu.au

Data availability

Amplicon and shotgun metagenomic sequences are available on NCBI's Sequence Read Archive (BioProject accession: PRJNA1248654).

Acknowledgements

This study was supported by a grant from the Australian Research Council (ARC-DP210102176). Experimental procedures were approved by the Animal Ethics Committee of Charles Darwin University, Australia (permit A21010). Sampling was conducted under a permit from the Puerto Rico government (2022-IC-054) and permission from Jardín Botánico (Universidad de Puerto Rico) and Hacienda la Esperanza (Para la Naturaleza). Samples were imported into Australia under permit 0007182743. Thanks to Ana Longo and Cameron Hudson for site suggestions in Hawaii and Puerto Rico, Alex Griffiths and Katie Gorman for sampling assistance in Hawaii, and Richard Thomas for assistance in Puerto Rico. Thanks to Mirjam Kaestli for valuable discussion on handling shotgun metagenomics data.

Author contributions (**CRediT)**

C Weitzman: conceptualisation, data curation, formal analysis, investigation, visualisation, writing – original draft, writing – review & editing

K Day: investigation, writing – review & editing

G Brown: conceptualisation, funding acquisition, investigation, writing – review & editing

K Gibb: conceptualisation, funding acquisition, resources, writing – original draft, writing – review & editing

K Christian: conceptualisation, funding acquisition, investigation, resources, supervision, writing – original draft, writing – review & editing

ABSTRACT

Host-associated microbial communities are shaped by environmental availability, host filtering, microbial interactions, and prior pathogen exposure, with connected habitats promoting greater adaptive microbiome potential. Across the invasive range of cane toads, containing expansive disconnects between populations, we found strong spatial variation in skin bacterial communities, including among nearby sites, and high within-site variability in alpha and beta diversity. Communities were moderately unbalanced, with many low-abundance, highly transient taxa likely contributing to instability and divergence among individuals. Despite this variability, we detected persistent core taxa across broad spatial and temporal scales, suggesting potential functional importance, though their ubiquity in the environment versus host selection remains unresolved. Network analyses showed that keystone taxa typically had low abundance and showed little overlap with core members, indicating that core and keystone concepts may capture distinct facets of microbiome structure. Although taxonomic composition varied widely, functional profiles were more similar among sites, consistent with functional redundancy. Neither functional nor taxonomic patterns aligned with climate, invasion history, or host evolutionary change, emphasising the dominant roles of local environments, microbial reservoirs, and individual host movement in shaping cane toad skin microbiomes.

Keywords: *Rhinella marina*, skin bacteria, spatial patterns, invasion

INTRODUCTION

Amphibians can have important ties with their skin bacteria, aiding host resilience in facing environmental stressors and invading pathogens (Woodhams et al. 2014, Rebollar et al.

2016, 2020, Fontaine and Kohl 2023). Feedback between amphibian hosts and their skin communities can lead to selection for bacterial community members (Loudon et al. 2016), which presumably impacts the similarities and shared members found across widespread host populations (e.g., Christian et al. 2018, Loudon et al. 2020). However, species also exhibit natural variation in bacterial community membership and composition, including diverging microbiome diversity across space (Kueneman et al. 2014, Christian et al. 2018, Weitzman et al. 2026). Free-ranging amphibians acquire their skin bacteria from the environment (Loudon et al. 2014, Walke et al. 2014), and consequently, host populations may have differing communities due to direct environmental inputs. These interactions are likely further impacted by variation and changes in intrinsic host factors and selective processes that control bacterial colonisation, growth, and persistence. Widespread species, particularly invasive species inhabiting broad environments, provide opportunities to parse the relative influences of maintained, fundamental microbiome characteristics (and characters) and modifications to those communities over space, time, and habitats.

Among invasive amphibians, few have been studied to the extent of cane toads (*Rhinella marina*). Native to Central and South America, cane toads have been introduced into many habitats worldwide—with varying success—often in attempt to reduce insect pests (Lever 2001, Turvey 2013). The species' invasion from the Americas across the Pacific Ocean to Australia occurred from a single translocation to Queensland less than 100 years ago, scattered in sugar cane fields near the city of Cairns in 1935 (Turvey 2013). Their recent spread between and across continents has allowed for real-time observations of cane toads' expansion into suitable habitats and examinations of evolutionary and plastic morphological and physiological

changes enabling the toad's Australia-wide range expansion with respect to immune function (Brown et al. 2015), morphology (Hudson et al. 2016), reproduction (Hudson et al. 2015), and dispersal (Shine et al. 2021). Cane toads also provide a model system to address the taxonomic and functional differences in skin microbiomes across space. Despite high transience of low-abundance taxa in the communities and large temporal shifts in diversity, cane toads nevertheless harbour core (i.e., present in a high proportion of individuals) communities both across time and space (Christian et al. 2018, Weitzman et al. 2023, 2025). In an effort to determine drivers of community diversity, it may be useful to establish whether core community members are also keystone taxa, i.e., they have a disproportionate influence on community structure, and thus may impact community function (Lynch and Neufeld 2015, Banerjee et al. 2018). The overlap between core and keystone taxa is important, as keystone bacteria may include rare or low-abundance taxa, but would have greater influence when present in more communities (Lynch and Neufeld 2015, Banerjee et al. 2018).

Distinct communities across space and time despite core taxa begs the question, to what degree is community composition seemingly random? Few community similarities on the level of amplicon sequence variants (ASVs) could be a consequence of differing taxa available for colonisation. However, previous work relaxing the taxonomic level of inquiry from unique reads to clusters of similar reads (operational taxonomic units) revealed that the variation among individuals and locations is not largely explained by microdiversity in available environmental bacteria (Weitzman et al. 2023). Alternatively, rather than requiring specific members in microbiomes, functional redundancy may explain taxonomic variation among communities (Belden et al. 2015; Louca et al. 2018).

111 We use cane toads (*Rhinella marina*) and their vast invaded range as a model system to
112 study spatial patterns in their skin microbial structural and functional diversity. Introductions of
113 cane toads to Puerto Rico, Hawaii, and Australia were a failed attempt to control populations of
114 cane beetles infesting sugarcane plantations. Cane toads were first introduced to Puerto Rico
115 via two releases in the early 1920s of toads collected from Jamaica and Barbados, which had
116 been colonised ~100 years prior by toads from Guyana (Lever 2001, Turvey 2013). Introductions
117 into Puerto Rico were at the Rio Piedras experimental station in San Juan, a site run by the
118 University of Puerto Rico at the university's Botanical Garden. From 1932-1934, toads were
119 introduced to Hawaii via the island of Oahu and distributed from there after given a chance to
120 produce the 100,000s of offspring required to supply the sugar plantations of the islands
121 (Turvey 2013). In mid-1935, toads collected in Honolulu, Oahu were transported to
122 Queensland, Australia, allowed to reproduce in captivity, and released into the wild, beginning
123 their devastating journey of invasion across Australia. Today, their invaded range in Australia
124 extends south down the length of Queensland into New South Wales, and west across northern
125 Australia to the west coast (Broome, Western Australia).
126 We explored spatial patterns of skin bacterial communities on cane toads in their
127 invaded range, representing five geographic regions and the species' invasion route from the
128 Caribbean, to Hawaii, and across northern Australia. A combination of amplicon and shotgun
129 metagenomic sequencing data allowed us to address the overarching goal of assessing
130 similarities among community structure, community function, and putatively important taxa on
131 cane toads to discern the extent of bacterial persistence on this host species across its
132 extensive range. The data and analyses in the present study expand on our previous work

(Weitzman et al. 2023, 2025) to detect similarities of toad skin communities despite their expected differences. Here, we evaluate three hypotheses: (H1) In support of previous results from Australia (Weitzman et al. 2023), cane toads at different sites host bacterial communities with different structure (taxonomic differences, assessed with amplicon data). (H2) Despite those differences, toads nevertheless harbour keystone taxa that match core bacteria shared among the host sites, indicating retention of their functional importance in the communities. (H3) Toads at different sites host similar functional communities (inferred from metagenomic data), suggesting conserved functional relationships between the microbes and their host across space. These data were further used to explore correlations between structural and functional communities. Alongside these questions, we compare our results with previous cane toad samples to identify persistent bacteria across space and time.

METHODS

Study system and sampling

We studied spatial patterns in skin bacteria on wild toads from nine invaded locations (sites) in Puerto Rico, Hawaii, and across Australia (Table 1), grouped into five regions: Puerto Rico (N = 2 sites, 50 km apart), Hawaii (N = 2 sites on different islands, 225 km apart as the crow flies), Queensland (Australia; N = 2 sites, 32 km apart near the original site of toad release in 1935), Northern Territory (N = 1 site), and Western Australia (N = 2 sites, 408 km apart). Sampling two sites from most regions allowed us to detect short-range site-level differences in communities. Due to logistical limitations, we were unable to sample from the region of South America that was used as a source for toads that invaded the Caribbean. Samples were

collected from May 2022 to May 2023.

Individuals were hand-captured in the field at night, with swab samples collected the night of capture before release. Briefly, individuals were rinsed with 100 mL distilled water and swabbed with a sterile flocked swab (Copan FLOQSwabs, Copan Diagnostics Inc., Murrieta, CA, USA) with 30 strokes around the body as previously described (Weitzman et al. 2025). During each evening of sampling, we also collected an environmental control sample for filtering contaminant reads from the 16S rRNA dataset (see below). A new pair of gloves was used by the handler for each toad to minimise cross-contamination. Swabs were preserved in 300 µL Zymo DNA/RNA Shield (Zymo Research, Irvine, CA, USA), stored on ice in the field, and frozen at –20 ˚C upon return to the lab until DNA extraction. After swabbing, toads were measured (mass; snout-vent length, SVL) and sexed. DNA from swab samples was extracted with the Norgen Microbiome Kit (Norgen Biotek Corp., Thorold, ON, Canada). Samples were DNA-extracted in batches, with DNA extraction groups including samples from at least three separate sites.

Amplicon sequencing and data processing

Library prep of a portion of the V4 region of bacterial 16S rRNA gene was conducted at the Ramaciotti Centre for Genomics with the Earth Microbiome Project 515F/806R primers (Caporaso et al. 2011, Apprill et al. 2015, Parada et al. 2016). Amplicon sequencing was performed on an Illumina NextSeq-1000 with 2×300bp chemistry alongside additional samples from other anurans. Due to low reverse read quality, data processing and analyses were conducted on the forward reads.

With DADA2 in QIIME 2024.2 (Callahan et al. 2016, Bolyen et al. 2019), reads were trimmed (36bp) and truncated (290bp), and amplicon sequence variants (ASVs) were identified. Taxonomy of ASVs was classified with sklearn using the 515/806 classifier based on the Silva 138 database (Pedregosa et al. 2011, Quast et al. 2012, Yilmaz et al. 2014). After removing data from other studies, we used the *decontam* package in RStudio (Davis et al. 2018, R Core Team 2023, RStudio Team 2023) to identify potential contaminant reads based on eight control samples collected and extracted alongside toad samples (swabs exposed to water, air, and gloves at eight of the sampling locations). Using the prevalence method and default threshold of 0.1, 0.11% of ASVs were identified as contaminants and removed from the dataset. After excluding the control samples, further potential spurious taxa were filtered out, including those that never reached a relative abundance of 0.05% in a single sample, and those present in only one sample (Reitmeier et al. 2021). Core and keystone taxa were identified based on all samples beginning with a non-normalised (non-rarefied) dataset. For analyses of diversity, we evaluated rarefaction curves before removing the sample with lowest reads and normalising to 26,111 reads per sample, removing a sample from Kurrimine Beach that did not reach an asymptote in rarefaction analysis.

Amplicons – Patterns in bacterial taxa

With amplicon data, we analysed three diversity metrics—alpha: richness and evenness; and beta: Bray–Curtis dissimilarity—to evaluate drivers of community diversity on toad skin and address H1. Variables of interest included four location-based values: site, region, longitude, and east-to-west site order (1 = Botanical Garden in Puerto Rico, 9 = Fitzroy Crossing in WA;

Table 1); three toad metrics: snout-vent length (SVL), mass, and sex (male or female, removing ten toads of unknown sex); and DNA extraction group to account for effects of sample handling. For each diversity metric, we used a model selection approach to identify the best fit drivers of diversity in the samples. Analyses were conducted in R on N = 213 samples with complete metadata. With the *AICcPermanova* package (Corcoran 2023), we generated all model possibilities and filtered out models with high multicollinearity among predictors (default maximum variance inflation factor of 5), resulting in 32 models tested. The selected models were those with ΔAICc < 2 from the top model, but we present results of the top five models for context.

Alpha diversity metrics were analysed with linear models (log-transformed for ASV evenness), with AICc values calculated in the *MuMIn* package (Bartoń 2025), partial p-values calculated with the *car* package (Fox and Weisberg 2019), and post-hoc pairwise comparisons in *emmeans* (Lenth and Piaskowski 2025). Beta-diversity metrics were analysed with permutational MANOVAs (PERMANOVAs) in *AICcPermanova*. Due to the importance of toad site in beta diversity, we further analysed beta dispersion among sites with the *vegan* package (Oksanen et al. 2025) and conducted pairwise comparisons between sites in *RVAideMemoire* (Hervé 2025).

To identify relatively important, keystone bacteria on cane toads and assess H2, keystone ASVs were inferred by constructing a SPRING network (Yoon et al. 2019) with the *NetCoMi* and *phyloseq* packages (McMurdie and Holmes 2013, Peschel 2025). Network construction was conducted on the 500 ASVs with $\lambda = 50$ and 50 repeated subsamples. Hubs (i.e., keystone taxa) were identified based on eigenvector centrality. Distinct from the aim of

identifying “keystone” taxa with putative importance, we further identified “core” taxa, those found in high proportions of communities. Here, we define core ASVs for each site as those present in at least 90% of the samples, and then determine the overlap of keystone and core bacteria.

This study focuses on results from bacterial ASVs, while further results from bacterial genera are available in the supplemental materials.

Shotgun metagenomics – Sequencing and data processing

A subset of samples representing one site from each region (N = 7 samples from each of the Botanical Garden, Wailuhu, Innisfail, Middle Point, and Fitzroy Crossing) were subjected to shotgun metagenomics sequencing at Ramaciotti Centre for Genomics on an Illumina NovaSeq X Plus with 2×150 bp chemistry. Samples for shotgun metagenomics were chosen prioritising samples with lower within-site average Bray–Curtis distances, representing at least three males and three females per sampling site, and removing small (< 80 mm) toads.

Using trimmomatic (Bolger et al. 2014), adapters were removed from paired-end reads, a sliding window method removed low-quality sequence segments (average quality threshold of 20 across 5 bases), low-quality (quality < 3) leading and trailing bases were removed, and final reads at least 50 bases long were kept. We used bowtie2-build to create a Bowtie index from a concatenated file of PhiX and cane toad (https://www.ebi.ac.uk/ena/browser/view/GCA_900303285.2) genomes to utilize Bowtie2 v2.4.3 (Langmead and Salzberg 2012) to remove those non-target reads. Using samtools v1.16.1 (Li et al. 2009), sam files were converted to bam files, unmapped reads were retained, and

forward and reverse reads were sorted. Sorted reads were converted back to fastq files with bedtools v2.30.0 (Quinlan and Hall 2010). Compressed fastq.gz files of host-removed reads were uploaded to Galaxy Australia (The Galaxy Community 2024) for further processing. Reads for each sample were assembled into contigs using MEGAHIT v1.2.9 (Li et al. 2015) with minimum length of output contigs of 200 bases, minimum, maximum, and step increment of k-mer sizes of 21, 91, and 12, respectively, and otherwise default parameters. Open reading frames were predicted in Prodigal v2.6.3 (Hyatt et al. 2010) with the "meta" mode, and CD-HIT (Li and Godzik 2006, Fu et al. 2012) was used to cluster protein translations based on 95% sequence identity. EggNOG-mapper v5.0.2 (Huerta-Cepas et al. 2016, 2017) provided functional annotations of the representative protein sequences, computing seed orthologs with DIAMOND (Buchfink et al. 2021) and employing Diamond's "very-sensitive" mode. We kept ortholog groups matching Bacteria for analysis.

Shotgun metagenomics – Patterns in bacterial function

To identify differences in microbial community function among toads (H3), we used the *vegan* package in R to create an Aitchison distance matrix of KEGG orthology (counts per sample with pseudocount of 1, removing unassigned reads) and used a PERMANOVA (adonis2) to sequentially analyse the effects of toad site and sex with 999 permutations. Data were also collapsed based on assigned KEGG modules and clusters of orthologous genes (COG) functional groups, separately, with each analysed with a PERMANOVA of Aitchison distances as with KEGG orthology above. Pairwise PERMANOVAs assessed pairwise differences between toad sites for each metric.

Differential read counts were analysed among the toad sites with the DESeq2 package (Love et al. 2014) for KEGG orthology, KEGG modules, and COGs, separately, with false-discovery rate (FDR) p-value adjustment.

Comparing structure and function

We used Mantel tests to detect correlations between community structure (beta diversity of ASV data) and the three levels of community function. Beta-diversity data were subset to include the samples subjected to shotgun metagenomic sequencing. Mantel tests were performed with the *vegan* package, comparing the distance matrix of beta diversity with that of KEGG orthology, KEGG modules, and COGs, separately. These tests were performed with and without the block strata option to account for site-level differences.

RESULTS

Bacterial diversity differs among geographical sites

The final amplicon dataset included 5,108 ASVs and an average of 139,966 $\pm$ 59,247 (range 16,392–363,178) reads per sample. Normalising the dataset removed one ASV from analyses.

In support of H1, toad site was a strong predictor of both metrics of alpha diversity (Table 2, Figure 1). For evenness, other top models also included region, toad size (SVL), and sex, though toad sex was not statistically significant. Richness varied considerably both within and between sites (Figure 1a). In contrast, evenness differed less among sites and regions (Figure 1b–c), and it tended to increase in larger toads (Figure S1).

Similarly, model selection of beta diversity (Table 3, Figure 2) found that toad site alone was the best predictor, accounting for 38% of the variation. All nine sampling sites differed from each other in pairwise tests, and the sites also differed in beta dispersion ($p = 0.001$).

Little overlap between keystone and core bacteria

There were 25 keystone ASVs (Figure 3a), of which 12 also appeared as core ASVs in at least one site, although most of them were present at very low relative abundances. Across all sites, 344 ASVs were part of the core community in at least one toad site, and most of these were also low-abundance taxa (Figure 3b). The core communities included 13 ASVs that occurred in every sample. These belonged to unidentified Micrococcales (five ASVs), *Niabella* (four ASVs), and one ASV each from *Aestuariimicrobium*, *Microbacterium*, *Antricoccus*, and an unidentified Propionibacteriaceae. UpSet plots showing how core taxa are shared among sites are provided in the supplemental materials (Figures S4, S5). Notably, none of the 17 ASVs that were core in all nine sites were identified as keystone ASVs.

Variability in functional profiles across toad sites

Shotgun metagenomics sequencing resulted in 1,222,579,184 total reads. On average, 85% of reads per sample passed quality filtering and removal of host-associated DNA. The 59,452–666,339 contigs per sample were identified as 496,789 bacterial seed orthologs, including 6,711 KEGG orthologs, 599 KEGG modules, and 23 COG categories (within each grouping, seed orthologs not identified were removed).

Although the overall proportions of COG categories were similar across samples (Figure 4), toad site predicted all three measures of bacterial function, explaining about 20–30% of the variation (Table 4). When comparing sites pairwise, differences were fewer with broader functional groupings. Finer-scale community function (KEGG orthology) was similar between Botanical Garden (PR) and Innisfail (QLD), and between Wailuku (HI) and Middle Point (NT); all other pairs differed (visible in ordinations, Figure 5a). For KEGG modules, half of the pairwise comparisons were significant: Botanical Garden communities were similar to the three Australian sites but different from Wailuku; Wailuku matched Middle Point but not the other two Australian sites; and within Australia, only Fitzroy and Innisfail were similar (Figure 5b). COG-based functions showed no pairwise differences among sites (Figure 5c). Because some sites had small sample sizes, we cannot tell whether the higher functional variation seen in certain sites reflects sampling or is typical in the field.

We found no significant differences in KEGG orthologs, KEGG modules, and COGs among the toad sites.

No correlation between ASV communities and function

There were no significant relationships between ASV-level community structure and community function (Table 5), however, correlations were found in genus-level analyses (Table S3).

DISCUSSION

Variability in host microbial communities results from many factors, including environmental diversity (availability), filtering by the host (skin chemistry), interactions among the microbes themselves, and previous exposure to pathogens (Doolin and Woodhams 2026, Medina et al. 2026). In this study, we have explored variation in microbial communities across vast distances, including continental-scale disconnects between populations, with particular emphasis on the concepts of core and putative keystone constituents. The lack of overlap between these two components of the skin microbiome may require a re-evaluation of their significance.

Structural and taxonomic communities

As predicted, cane toads at different sites hosted structurally different bacterial communities on their skin, supporting our previous work from Australia (Weitzman et al. 2023). Interestingly, even toads from nearby sites had distinct communities, and there was high variability within and among sites in both alpha and beta diversity. Evenness in these samples indicated moderately unbalanced communities on these toads. In this case, communities included many low-relative-abundance taxa and few high-abundance taxa. Previously, we learned that taxa on cane toads with low relative abundance were extremely transient, meaning they were less likely to remain on a host over time (Weitzman et al. 2025). These bacteria with high transience will affect the differences we find between individuals within and between populations. Indeed, high diversity can impede community stability (Ellison et al. 2021). Importantly, cane toads are highly mobile (Shine et al. 2021), picking up diverse bacteria from the bacterial reservoirs in the broad habitats they encounter (Loudon et al. 2014, Walke et

al. 2014, Weitzman et al. 2025), enabling regular colonisation of both transient and more persistent bacteria. Even while sharing the same environment, stochastic colonisation and extinction can lead to multiple possible community states and markedly different skin communities on individuals in the same population (Chase and Myers 2011). Consequently, very localised patterns in bacterial availability and host-specific effects should play a role in spatial differences and variability among individuals.

Fine-scale environmental drivers likely impacted the data we collected and may explain some of our results, but our focus on long-distance community similarities on cane toads did not allow for this type of analysis. Bioclimate has been found to correlate with skin community richness across broad amphibian taxa and sites (Kueneman et al. 2019), however, the differences we found in richness between nearby sites do not support that pattern. Nevertheless, our data may very well fit within the high level of noise (i.e., variability) in the previous study (Kueneman et al. 2019). Within single host species, others have also detected environmental drivers of diversity by sampling in more localised areas (e.g., Becker et al. 2017, Albecker et al. 2019, Lucia et al. 2024). Beyond these differences among hosts, their transient taxa, and environmental influences on diversity, we did indeed find persistence in community members in this widespread sampling, but our data suggest that while persistent, the more influential keystone community members are some of the less abundant, less persistent bacteria.

Although we predicted a correspondence between keystone and core bacteria, we found little overlap on cane toads, and keystone taxa generally had low abundance. These analyses provide direction for bacteria to further investigate regarding their community

373 importance, such as *Nocardioides* and *Variovorax* spp. (Figure 3, S3). While low abundance and
374 rarity do not negate their impact, keystone bacteria would have greater influence when present
375 in more communities (Lynch and Neufeld 2015, Banerjee et al. 2018). Our analysis identified
376 keystone taxa as those strongly affecting network structure. Consequently, whether less
377 volatile, persistent bacteria present on most or all individuals are also keystone community
378 members may not be detected with this method, as there are no representative communities
379 where they are missing.

380 Alongside core bacteria in this spatial sampling scheme, we compared data from these
381 samples with those from temporal sampling at our Middle Point, Australia site (Weitzman et al.
382 2025). These shared core taxa comprised many of the reads among the samples (Tables S4-S7).
383 The robust, shared taxa across space and time on cane toads suggests a retention of their
384 functional importance. If the bacterial microbiome is a definitive characteristic of toads (think
385 enzymes in the toad endocrine system), then we might expect even more persistence. On the
386 other hand, given the huge sampling distances and presumably different environmental
387 microbial communities, coupled with the possibility of different microbes performing the same
388 function (Louca et al. 2018), maybe it's a wonder that there are any persistent bacteria at all.
389 Here, we cannot tease apart whether these taxa reflect some level of importance in the
390 microbiome and selection by the host (Loudon et al. 2016) or simply the ubiquity of these
391 microbes.

392

393 *Where structure meets function*

Thus far, we have discussed the variable taxonomic communities on cane toads across their invaded range, which is found regardless of some persistent taxa that may play a stabilising functional role. If we predict that cane toads interact with their skin microbiomes, and those microbes play a function for the host (beyond simply their physical presence), then we could expect that the functional community itself is stable among hosts and populations despite divergent community structures. Certainly, there is functional redundancy in bacterial communities (Louca et al. 2018). Cane toads did harbour more similar functional diversity than taxonomic diversity, with fewer differences between sites, but there was no discernable pattern among our results. Deeper exploration found no correlation between ASV diversity and functional diversity, suggesting that variable structural communities can result in similar functional communities. At the genus level, however, there was a relationship between community structure and function, which could be influenced by microdiversity and ASVs in the same genus performing the same function, as widespread lineages can have strain-level turnover among sites or hosts (Larkin and Martiny 2017, García-García et al. 2019). Importantly, our methods identified the broad bacterial functional diversity, though many of these functions we may not expect to align among communities if they are not important to the host. Just as core taxa persist despite differing community structure and composition, important functionality may persist despite differing functional diversity, as is the case for gene functions with protective effects against disease in other amphibians (Martínez-Ugalde et al. 2024).

Frequent exposure to challenges such as pathogens facilitates the retention of pathogen-inhibiting components of the microbiome and promotes stability of the community. The expansive range of cane toads across northern Australia spans the range of chytrid fungus

(due to thermal constraints in some parts of the toads' range), where there are fewer pathogen-inhibiting microbes in the absence of chytrid compared to the microbiome of toads inhabiting parts of their range where chytrid is found (Weitzman et al. 2019). Thus, site-specific pathogen pressures, whether due to habitat fragmentation or clinal climatic factors, can influence variability in host microbial communities.

Where there were similarities in functional diversity between cane toad sites, those sites did not represent any obvious pattern in environment, including climate and weather (e.g., similarities between Wailuku, Hawaii and Middle Point, Australia). The pattern of functional communities further did not indicate a signal of evolutionary changes to the toads themselves, which could drive selection for particular community functions (parallel to other changes observed in toad morphology and physiology), which would have been observed through increased dissimilarities between more distant sites from Puerto Rico to Fitzroy Crossing. As there were also no structural, taxonomic patterns that would support an invasion-route series of changes, these results highlight the importance of local environment, bacterial reservoirs, and individual host factors (such as movement across the landscape) in this system.

Conclusions

Cane toads have invaded tropical and temperate regions across multiple continents. In their spread from east to west across Australia, multiple phenotypical changes have supported their incursion into new territory, such as behavior (Gruber et al. 2017), locomotor performance (Kosmala et al. 2017), and morphology (Hudson et al. 2021). However, when it comes to their skin bacteria, rather than exhibiting geographical patterns, communities are

comprised of taxa filtered from their environment, including some persistent bacteria found on toads regardless of where they are in the world. These abundant, recurring taxa point to where future microbial ecology studies should focus to discern the extent of importance and interaction cane toads have with their skin communities. As higher taxonomic levels of bacteria correlate with functional profiles, this may suggest prevailing function of toad skin microbes. Indeed, functional communities were more similar among toads than the taxonomic communities that shape them.

This partial decoupling of structure and function highlights the likely role of functional redundancy in maintaining microbiome-mediated services across heterogeneous environments. In addition, the weak correspondence between core and keystone members, and the low abundance of many keystone taxa, suggest that ecological influence within these communities is not simply a function of prevalence or persistence, and that network-based “importance” may overlook ubiquitous, host-selected bacteria. Together, these findings emphasise that predictions about host–microbiome interactions, adaptive microbiome potential, and disease mitigation in invasive species must account for both the dynamic, stochastic nature of community assembly and the possibility that critical functions can be maintained by different taxa in different places. Future work integrating experimental manipulations, finer-resolution environmental data, and host trait measurements will be essential for determining when persistent or keystone taxa, versus emergent community-level properties, are the primary drivers of microbiome function and host health.

References

460 Albecker, M. A., L. K. Belden, and M. W. McCoy. 2019. Comparative analysis of anuran
461 amphibian skin microbiomes across inland and coastal wetlands. Microbial Ecology
462 78:348–360.
463 Apprill, A., S. McNally, R. Parsons, and L. Weber. 2015. Minor revision to V4 region SSU rRNA
464 806R gene primer greatly increases detection of SAR11 bacterioplankton. Aquatic
465 Microbial Ecology 75:129–137.
466 Banerjee, S., K. Schlaeppi, and M. G. Van Der Heijden. 2018. Keystone taxa as drivers of
467 microbiome structure and functioning. Nature Reviews Microbiology 16:567–576.
468 Bartoń, K. 2025. MuMIn: Multi-Model Inference. R package version 1.48.11.
469 Becker, C. G., A. V. Longo, C. F. B. Haddad, and K. R. Zamudio. 2017. Land cover and forest
470 connectivity alter the interactions among host, pathogen and skin microbiome.
471 Proceedings of the Royal Society B: Biological Sciences 284:20170582.
472 Belden, L. K., M. C. Hughey, E. A. Rebollar, T. P. Umile, S. C. Loftus, E. A. Burzynski, K. P. C.
473 Minbiole, L. L.. House, R. V. Jensen, M. H. Becker, J. B. Walke, D. Medina, R. Ibáñez, and
474 R. N. Harris. 2015. Panamanian frog species host unique skin bacterial communities.
475 Frontiers in Microbiology 6:1171.
476 Bolger, A. M., M. Lohse, and B. Usadel. 2014. Trimmomatic: a flexible trimmer for Illumina
477 sequence data. Bioinformatics 30:2114–2120.
478 Bolyen, E., J. R. Rideout, M. R. Dillon, N. A. Bokulich, C. C. Abnet, G. A. Al-Ghalith, H. Alexander,
479 E. J. Alm, M. Arumugam, F. Asnicar, Y. Bai, J. E. Bisanz, K. Bittinger, A. Brejnrod, C. J.
480 Brislawn, C. T. Brown, B. J. Callahan, A. M. Caraballo-Rodríguez, J. Chase, E. K. Cope, R.
481 Da Silva, C. Diener, P. C. Dorrestein, G. M. Douglas, D. M. Durall, C. Duvallet, C. F.

Edwardson, M. Ernst, M. Estaki, J. Fouquier, J. M. Gauglitz, S. M. Gibbons, D. L. Gibson, A. Gonzalez, K. Gorlick, J. Guo, B. Hillmann, S. Holmes, H. Holste, C. Huttenhower, G. A. Huttley, S. Janssen, A. K. Jarmusch, L. Jiang, B. D. Kaehler, K. B. Kang, C. R. Keefe, P. Keim, S. T. Kelley, D. Knights, I. Koester, T. Kosciolek, J. Kreps, M. G. I. Langille, J. Lee, R. Ley, Y.-X. Liu, E. Loftfield, C. Lozupone, M. Maher, C. Marotz, B. D. Martin, D. McDonald, L. J. McIver, A. V. Melnik, J. L. Metcalf, S. C. Morgan, J. T. Morton, A. T. Naimey, J. A. Navas-Molina, L. F. Nothias, S. B. Orchanian, T. Pearson, S. L. Peoples, D. Petras, M. L. Preuss, E. Pruesse, L. B. Rasmussen, A. Rivers, M. S. Robeson, P. Rosenthal, N. Segata, M. Shaffer, A. Shiffer, R. Sinha, S. J. Song, J. R. Spear, A. D. Swafford, L. R. Thompson, P. J. Torres, P. Trinh, A. Tripathi, P. J. Turnbaugh, S. Ul-Hasan, J. J. J. van der Hooft, F. Vargas, Y. Vázquez-Baeza, E. Vogtmann, M. von Hippel, W. Walters, Y. Wan, M. Wang, J. Warren, K. C. Weber, C. H. D. Williamson, A. D. Willis, Z. Z. Xu, J. R. Zaneveld, Y. Zhang, Q. Zhu, R. Knight, and J. G. Caporaso. 2019. Reproducible, interactive, scalable and extensible microbiome data science using QIIME 2. Nature Biotechnology 37:852–857.

Brown, G. P., B. L. Phillips, S. Dubey, and R. Shine. 2015. Invader immunology: invasion history alters immune system function in cane toads (*Rhinella marina*) in tropical Australia. Ecology Letters 18:57-65.

Buchfink, B., K. Reuter, and H.-G. Drost. 2021. Sensitive protein alignments at tree-of-life scale using DIAMOND. Nature Methods 18:366–368.

Callahan, B. J., P. J. McMurdie, M. J. Rosen, A. W. Han, A. J. A. Johnson, and S. P. Holmes. 2016. DADA2: High-resolution sample inference from Illumina amplicon data. Nature Methods 13:581–583.

Caporaso, J. G., C. L. Lauber, W. A. Walters, D. Berg-Lyons, C. A. Lozupone, P. J. Turnbaugh, N. Fierer, and R. Knight. 2011. Global patterns of 16S rRNA diversity at a depth of millions of sequences per sample. Proceedings of the National Academy of Sciences 108:4516–4522.

Chase, J. M., and J. A. Myers. 2011. Disentangling the importance of ecological niches from stochastic processes across scales. Philosophical transactions of the Royal Society B: Biological sciences 366:2351–2363.

Christian, K., C. Weitzman, A. Rose, M. Kaestli, and K. Gibb. 2018. Ecological patterns in the skin microbiota of frogs from tropical Australia. Ecology and Evolution 8:10510–10519.

Corcoran, D. 2023. AICcPermanova: Model Selection of PERMANOVA Models Using AICc.

Davis, N. M., D. M. Proctor, S. P. Holmes, D. A. Relman, and B. J. Callahan. 2018. Simple statistical identification and removal of contaminant sequences in marker-gene and metagenomics data. Microbiome 6:226.

Doolin, M. L., and D. C. Woodhams. 2026. Advancing the study of microbial symbionts of amphibians and reptiles. Frontiers in Amphibian and Reptile Science 4:1810202.

Ellison, S., R. Knapp, and V. Vredenburg. 2021. Longitudinal patterns in the skin microbiome of wild, individually marked frogs from the Sierra Nevada, California. ISME Communications 1:45.

Fontaine, S. S., and K. D. Kohl. 2023. The microbiome buffers tadpole hosts from heat stress: a hologenomic approach to understand host–microbe interactions under warming. Journal of Experimental Biology 226:jeb245191.

525 Fox, J., and S. Weisberg. 2019. An R Companion to Applied Regression, Third Edition. Thousand
526 Oaks CA: Sage.
527 Fu, L., B. Niu, Z. Zhu, S. Wu, and W. Li. 2012. CD-HIT: accelerated for clustering the next-
528 generation sequencing data. Bioinformatics 28:3150–3152.
529 García-García, N., J. Tamames, A. M. Linz, C. Pedrós-Alió, and F. Puente-Sánchez. 2019.
530 Microdiversity ensures the maintenance of functional microbial communities under
531 changing environmental conditions. The ISME Journal 13:2969–2983.
532 Gruber, J., G. Brown, M. J. Whiting, and R. Shine. 2017. Geographic divergence in dispersal-
533 related behaviour in cane toads from range-front versus range-core populations in
534 Australia. Behavioral Ecology and Sociobiology 71:38.
535 Hervé, M. 2025. RVAideMemoire: Testing and Plotting Procedures for Biostatistics. R package
536 version 0.9-83-12. Computer software.
537 Hudson, C. M., G. P. Brown, R. A. Blennerhassett, and R. Shine. 2021. Variation in size and shape
538 of toxin glands among cane toads from native-range and invasive populations. Scientific
539 Reports 11:936.
540 Hudson, C. M., G. P. Brown, and R. Shine. 2016. It is lonely at the front: contrasting evolutionary
541 trajectories in male and female invaders. Royal Society open science 3:160687.
542 Hudson, C. M., B. L. Phillips, G. P. Brown, and R. Shine, R. 2015. Virgins in the vanguard: low
543 reproductive frequency in invasion-front cane toads. Biological Journal of the Linnean
544 Society 116:743-747.

Huerta-Cepas, J., K. Forslund, L. P. Coelho, D. Szklarczyk, L. J. Jensen, C. von Mering, and P. Bork. 2017. Fast Genome-Wide Functional Annotation through Orthology Assignment by eggNOG-Mapper. Molecular Biology and Evolution 34:2115–2122.

Huerta-Cepas, J., D. Szklarczyk, K. Forslund, H. Cook, D. Heller, M. C. Walter, T. Rattei, D. R. Mende, S. Sunagawa, M. Kuhn, L. J. Jensen, C. von Mering, and P. Bork. 2016. eggNOG 4.5: a hierarchical orthology framework with improved functional annotations for eukaryotic, prokaryotic and viral sequences. Nucleic Acids Research 44:D286–D293.

Hyatt, D., G.-L. Chen, P. F. LoCascio, M. L. Land, F. W. Larimer, and L. J. Hauser. 2010. Prodigal: prokaryotic gene recognition and translation initiation site identification. BMC Bioinformatics 11:119.

Kosmala, G., K. Christian, G. Brown, and R. Shine. 2017. Locomotor performance of cane toads differs between native-range and invasive populations. Royal Society open science 4:170517.

Kueneman, J. G., M. C. Bletz, V. J. McKenzie, C. G. Becker, M. B. Joseph, J. G. Abarca, H. Archer, A. L. Arellano, A. Bataille, and M. Becker. 2019. Community richness of amphibian skin bacteria correlates with bioclimate at the global scale. Nature Ecology & Evolution 3:381–389.

Kueneman, J. G., L. W. Parfrey, D. C. Woodhams, H. M. Archer, R. Knight, and V. J. McKenzie. 2014. The amphibian skin-associated microbiome across species, space and life history stages. Molecular Ecology 23:1238–1250.

Langmead, B., and S. L. Salzberg. 2012. Fast gapped-read alignment with Bowtie 2. Nature methods 9:357–359.

567 Larkin, A. A., and A. C. Martiny. 2017. Microdiversity shapes the traits, niche space, and
568 biogeography of microbial taxa. Environmental Microbiology Reports 9:55–70.
569 Lenth, R. V., and J. Piaskowski. 2025. emmeans: Estimated marginal means, aka least-squares
570 means. R package version 2.0.1.
571 Lever, C. 2001. Cane Toad, the. Westbury Academic & Scientific Pub.
572 Li, D., C.-M. Liu, R. Luo, K. Sadakane, and T.-W. Lam. 2015. MEGAHIT: an ultra-fast single-node
573 solution for large and complex metagenomics assembly via succinct de Bruijn graph.
574 Bioinformatics 31:1674–1676.
575 Li, H., B. Handsaker, A. Wysoker, T. Fennell, J. Ruan, N. Homer, G. Marth, G. Abecasis, R. Durbin,
576 and 1000 Genome Project Data Processing Subgroup. 2009. The sequence
577 alignment/map format and SAMtools. bioinformatics 25:2078–2079.
578 Li, W., and A. Godzik. 2006. Cd-hit: a fast program for clustering and comparing large sets of
579 protein or nucleotide sequences. Bioinformatics 22:1658–1659.
580 Louca, S., M. F. Polz, F. Mazel, M. B. Albright, J. A. Huber, M. I. O'Connor, M. Ackermann, A. S.
581 Hahn, D. S. Srivastava, and S. A. Crowe. 2018. Function and functional redundancy in
582 microbial systems. Nature ecology & evolution 2:936–943.
583 Loudon, A. H., A. Kurtz, E. Esposito, T. P. Umile, K. P. C. Minbiole, L. W. Parfrey, and B. A.
584 Sheafor. 2020. Columbia spotted frogs (*Rana luteiventris*) have characteristic skin
585 microbiota that may be shaped by cutaneous skin peptides and the environment. FEMS
586 Microbiology Ecology 96:fiaa168.
587 Loudon, A. H., A. Venkataraman, W. Van Treuren, D. C. Woodhams, L. W. Parfrey, V. J.
588 McKenzie, R. Knight, T. M. Schmidt, and R. N. Harris. 2016. Vertebrate hosts as islands:

589 Dynamics of selection, immigration, loss, persistence, and potential function of bacteria
590 on salamander skin. Microbial Symbioses 7:333.
591 Loudon, A. H., D. C. Woodhams, L. W. Parfrey, H. Archer, R. Knight, V. McKenzie, and R. N.
592 Harris. 2014. Microbial community dynamics and effect of environmental microbial
593 reservoirs on red-backed salamanders (*Plethodon cinereus*). The ISME Journal 8:830–
594 840.
595 Love, M. I., W. Huber, and S. Anders. 2014. Moderated estimation of fold change and dispersion
596 for RNA-seq data with DESeq2. Genome Biology 15:550.
597 Lucia, Z., G. Giulio, G. Matteo, C. Stefano, L. P. Irene, P. Paolo, B. Giorgio, and H. C. Hauffe.
598 2024. More Than Meets the Eye: Unraveling the Interactions Between Skin Microbiota
599 and Habitat in an Opportunistic Amphibian. Microbial Ecology 87:176.
600 Lynch, M. D., and J. D. Neufeld. 2015. Ecology and exploration of the rare biosphere. Nature
601 Reviews Microbiology 13:217–229.
602 Martínez-Ugalde, E., V. Ávila-Akerberg, T. M. González Martínez, and E. A. Rebollar. 2024. Gene
603 functions of the Ambystoma altamirani skin microbiome vary across space and time but
604 potential antifungal genes are widespread and prevalent. Microbial Genomics 10.
605 McMurdie, P. J., and S. Holmes. 2013. phyloseq: an R package for reproducible interactive
606 analysis and graphics of microbiome census data. PLoS ONE 8:e61217.
607 Medina, D., R. A. Martins, P. R. Prist, S. Buttimer, W. J. Neely, L. K. Schuck, S. E. Greenspan, M. L.
608 Lyra, P. J. Kearns, D. C. Woodhams, and M. C. Bletz. 2026. Connecting habitats, boosting
609 disease resistance: Spatial connectivity enhances amphibian microbiome defenses

against fungal pathogen. Proceedings of the National Academy of Sciences 123:e2520745123.

Oksanen, J., G. L. Simpson, F. G. Blanchet, R. Kindt, P. Legendre, P. R. Minchin, R. B. O'Hara, P. Solymos, M. H. H. Stevens, E. Szoecs, H. Wagner, M. Barbour, M. Bedward, B. Bolker, D. Borcard, T. Borman, G. Carvalho, M. Chirico, M. de Caceres, S. Durand, H. B. A. Evangelista, R. FitzJohn, M. Friendly, B. Furneaux, G. Hannigan, M. O. Hill, L. Lahti, C. Martino, D. McGlinn, M.-H. Ouellette, E. Ribeiro Cunha, T. Smith, A. Stier, C. J. F. Ter Braak, and J. Weedon. 2025. vegan: Community Ecology Package.

Parada, A. E., D. M. Needham, and J. A. Fuhrman. 2016. Every base matters: assessing small subunit rRNA primers for marine microbiomes with mock communities, time series and global field samples. Environmental Microbiology 18:1403–1414.

Pedregosa, F., G. Varoquaux, A. Gramfort, V. Michel, B. Thirion, O. Grisel, M. Blondel, P. Prettenhofer, R. Weiss, V. Dubourg, J. Vanderplas, A. Passos, D. Cournapeau, M. Brucher, M. Perrot, and É. Duchesnay. 2011. Scikit-learn: Machine learning in Python. Journal of Machine Learning Research 12:2825–2830.

Peschel, S. 2025. NetCoMi: Network Construction and Comparison for Microbiome Data. R package version 1.2.0. https://netcomi.de.

Phillips, B. L., G. P. Brown, M. Greenlees, J. K. Webb, and R. Shine. 2007. Rapid expansion of the cane toad (*Bufo marinus*) invasion front in tropical Australia. Austral Ecology 32:169–176.

630 Quast, C., E. Pruesse, P. Yilmaz, J. Gerken, T. Schweer, P. Yarza, J. Peplies, and F. O. Glöckner.
631 2012. The SILVA ribosomal RNA gene database project: improved data processing and
632 web-based tools. Nucleic Acids Research 41:D590–D596.
633 Quinlan, A. R., and I. M. Hall. 2010. BEDTools: a flexible suite of utilities for comparing genomic
634 features. Bioinformatics 26:841–842.
635 R Core Team. 2023. R: A Language and Environment for Statistical Computing. R Foundation for
636 Statistical Computing, Vienna, Austria.
637 Rebollar, E. A., E. Martínez-Ugalde, and A. H. Orta. 2020. The amphibian skin microbiome and
638 its protective role against chytridiomycosis. Herpetologica 76:167–177.
639 Rebollar, E. A., S. J. Simonetti, W. R. Shoemaker, and R. N. Harris. 2016. Direct and indirect
640 horizontal transmission of the antifungal probiotic bacterium *Janthinobacterium lividum*
641 on green frog (*Lithobates clamitans*) tadpoles. Applied and Environmental Microbiology
642 82:2457–2466.
643 Reitmeier, S., T. C. A. Hitch, N. Treichel, N. Fikas, B. Hausmann, A. E. Ramer-Tait, K. Neuhaus, D.
644 Berry, D. Haller, I. Lagkouvardos, and T. Clavel. 2021. Handling of spurious sequences
645 affects the outcome of high-throughput 16S rRNA gene amplicon profiling. ISME
646 Communications 1:31.
647 RStudio Team. 2023. RStudio: Integrated Development Environment for R. RStudio, PBC.,
648 Boston, MA, USA.
649 Shine, R., R. A. Alford, R. Blennerhasset, G. P. Brown, J. L. DeVore, S. Ducatez, P. Finnerty, M.
650 Greenlees, S. W. Kaiser, S. McCann, and L. Pettit. 2021. Increased rates of dispersal of

free-ranging cane toads (*Rhinella marina*) during their global invasion. Scientific Reports 11:23574.

The Galaxy Community. 2024. The Galaxy platform for accessible, reproducible, and collaborative data analyses: 2024 update 52:W83–W94.

Turvey, N. 2013. Cane toads: a tale of sugar, politics and flawed science. Sydney University Press.

Walke, J. B., M. H. Becker, S. C. Loftus, L. L. House, G. Cormier, R. V. Jensen, and L. K. Belden. 2014. Amphibian skin may select for rare environmental microbes. The ISME Journal 8:2207–2217.

Weitzman, C. L., K. Day, G. P. Brown, K. Gibb, and K. Christian. 2025. Differential temporal shifts in skin bacteria on wild and captive toads. Microbial Ecology 88:35.

Weitzman, C. L., K. Day, K. M. Gorman, K. Gibb, G. P. Brown, and K. Christian. 2026. Little overlap in symbiotic bacteria of Coquí frogs in Hawaii and Puerto Rico. Biotropica 58:e70156.

Weitzman, C. L., M. Kaestli, K. Gibb, G. P. Brown, R. Shine, and K. Christian. 2019. Disease exposure and antifungal bacteria on skin of invasive cane toads, Australia. Emerging Infectious Diseases 25:1770-1771.

Weitzman, C. L., M. Kaestli, A. Rose, C. M. Hudson, K. Gibb, G. P. Brown, R. Shine, and K. Christian. 2023. Geographic variation in bacterial assemblages on cane toad skin is influenced more by local environments than by evolved changes in host traits. Biology Open 12:bio059641.

672 Woodhams, D. C., H. Brandt, S. Baumgartner, J. Kielgast, E. Küpfer, U. Tobler, L. R. Davis, B. R.
673 Schmidt, C. Bel, S. Hodel, and others. 2014. Interacting symbionts and immunity in the
674 amphibian skin mucosome predict disease risk and probiotic effectiveness. PLoS ONE
675 9:e96375.
676 Yilmaz, P., L. W. Parfrey, P. Yarza, J. Gerken, E. Pruesse, C. Quast, T. Schweer, J. Peplies, W.
677 Ludwig, and F. O. Glöckner. 2014. The SILVA and "all-species living tree project (LTP)"
678 taxonomic frameworks. Nucleic Acids Research 42:D643–D648.
679 Yoon, G., I. Gaynanova, and C. L. Müller. 2019. Microbial Networks in SPRING - Semi-parametric
680 Rank-Based Correlation and Partial Correlation Estimation for Quantitative Microbiome
681 Data. Frontiers in Genetics 10.
682

683 **Tables**

684 **Table 1** Sites of cane toad sampling in the USA and Australia. Site order is approximately in the
685 order of toad introduction, from east to west. N = 25 toads sampled from each site. Diversity N
686 = sample sizes for diversity analyses, removing samples with too few reads and samples from
687 toads with missing data. Introduction year is estimated based on Phillips et al. 2007, Turvey
688 2013, and more recently by direct observation.

689

Site	Region (abbreviation)	Latitude, Longitude	Introduction Year	Sampling Month	Diversity N
1 – San Juan Botanical Garden (Jardín Botánico de la UPR)	Puerto Rico, USA (PR)	18°23'33.42"N, 66° 3'20.27"W	1920-1925	Nov 2022	25
2 - Hacienda la Esperanza	Puerto Rico, USA (PR)	18°28'8.39"N, 66°31'28.03"W	1920-1925	Nov 2022	25
3 - Pahoa	Hawaii, USA (HI)	19°32'55.23"N, 154°54'11.22"W	1930-1935	Nov–Dec 2022	24
4 - Wailuku	Hawaii, USA (HI)	20°55'26.18"N, 156°29'36.64"W	1930-1935	Nov 2022	25
5 - Kurrimine Beach	Queensland, Australia (QLD)	17°47'4.87"S, 146° 5'56.15"E	~1935	May 2023	23
6 - Innisfail	Queensland, Australia (QLD)	17°29'36.53"S, 146° 4'36.39"E	~1935	May 2023	25
7 - Middle Point	Northern Territory, Australia (NT)	12°34'42.95"S, 131°18'51.91"E	2004-2005	May 2023	19
8 - Marlgu Billabong	Western Australia, Australia (WA)	15°32'58.16"S, 128°15'33.44"E	~2010-2015	May 2022	22
9 - Fitzroy Crossing	Western Australia, Australia (WA)	18°11'7.35"S, 125°35'2.13"E	2019	May 2022	25

690
691

692 **Table 2** Top five models identifying drivers of alpha diversity of bacterial ASVs on cane toad skin from linear models. *P*-value is

693 provided for each predictor. **Bold** denotes best model(s) for each metric based on ΔAICc < 2.

694

Models	AICc	ΔAICc	Model *P*	Site	Region	Longitude	SVL	Sex
ASVs, Richness								
Site	**2728.04**	**0**	**< 0.0001**	**<0.0001; $F_{(8,204)}$ = 31.78**				
Region + SVL	2832.08	104.0	< 0.0001		< 0.0001; $F_{(4,207)}$ = 17.01		0.06; $F_{(1,207)}$ = 3.48	
Region + SVL + Sex	2832.91	104.9	< 0.0001		< 0.0001; $F_{(4,206)}$ = 16.17		0.07; $F_{(1,206)}$ = 3.36	0.3; $F_{(1,206)}$ = 1.29
Region	2833.49	105.4	< 0.0001		< 0.0001; $F_{(4,208)}$ = 16.35			
Region + Sex	2834.19	106.2	< 0.0001		< 0.0001; $F_{(4,207)}$ = 15.40			0.2; $F_{(1,207)}$ = 1.40
ASVs, Evenness								
Site	**-305.33**	**0**	**0.004**	**0.004; $F_{(8,204)}$ = 2.98**				
Region + SVL	**-304.56**	**0.8**	**0.007**		**0.03; $F_{(4,207)}$ = 2.74**		**0.002; $F_{(1,207)}$ = 9.75**	
Region + SVL + Sex	**-304.36**	**1.0**	**0.007**		**0.02; $F_{(4,206)}$ = 3.07**		**0.002; $F_{(1,206)}$ = 9.54**	**0.2; $F_{(1,206)}$ = 1.91**
SVL	-302.00	3.3	0.02				0.02; $F_{(1,211)}$ = 5.22	
SVL + Longitude	-300.86	4.5	0.048			0.3; $F_{(1,210)}$ = 0.92	0.02; $F_{(1,210)}$ = 5.18	

695

Table 3 Beta diversity of bacteria on cane toad skin is strongly explained by host site. Top five permutational MANOVA models and R^2 for relevant predictors. **Bold** denotes best model based on ΔAICc < 2.

Models	AICc	ΔAICc	Site	Region	SVL	Mass	Sex
Site	**-451.57**	**0.0**	**0.379**				
Region + SVL + Sex	-417.82	33.8		0.206	0.021		0.014
Region + Mass + Sex	-416.40	35.2		0.205		0.016	0.015
Region + SVL	-416.04	35.5		0.219	0.021		
Region + Mass	-414.43	37.1		0.218		0.015	

Table 4 Shotgun metagenomics data were analysed with PERMANOVAs to determine the influences of toad site and sex on functional variation. For each data type, site and sex were analysed sequentially, with effects of sex assessed after accounting for site.

Predictor	***F (df)***	***R^2***	***P***
KEGG orthology			
Site	**3.02 (4,29)**	**0.288**	**0.001**
Sex	0.88 (1,29)	0.021	0.4
KEGG modules			
Site	**3.29 (4,29)**	**0.306**	**0.001**
Sex	0.86 (1,29)	0.020	0.4
COG categories			
Site	**1.73 (4,29)**	**0.190**	**0.04**
Sex	0.41 (1,29)	0.011	0.8

Table 5 Results of Mantel tests comparing community structure based on bacterial ASVs and three levels of community function. Significance values are provided with and without block strata to account for site-level differences.

Comparison	r	Significance (without strata)	Significance (with strata)
ASVs v KEGG orthology	0.125	0.1	0.2
ASVs v KEGG modules	0.105	0.2	0.2
ASVs v COGs	–0.078	0.7	0.8

Figure Captions

Figure 1 Richness (a) and evenness (b,c) of bacterial ASVs on cane toad skin by host location. Points provide raw data and are colour-coded by region for context. Bars are estimated marginal means and 95% confidence intervals. Differing letters above values in (a) denote toad sites with significantly different richness in pairwise tests. Asterisks indicate pairs of locations with significantly different evenness in pairwise tests.

Figure 2 Beta diversity (Bray–Curtis distances) of skin bacterial communities on cane toads differed by site. NMDS stress = 0.202. Points are average values per site, with rays ending at individual bacterial community values. Sites are colour-coded by region. Puerto Rico = pink. Hawaii = yellow. Queensland = green. Northern Territory = blue. Western Australia = purple.

Figure 3 Keystone and core bacteria in cane toad skin communities. Both were identified based on the full dataset, with n = 25 toad samples per site. (a) Keystone bacteria identified by

731 eigenvectors in a SPRING network. Colours denote the average relative abundance in the site.
732 White indicates the taxon was absent from that toad site. (b) Core bacterial ASVs (>90%
733 prevalence) subset to those representing on average > 2% relative abundance in at least one
734 relevant community. Colours denote average relative abundances per sampling site that the
735 taxon was present in the core community. White indicates the taxon was not core in the site
736 (i.e., it may have been present on some toads, but not in the site's core community). Asterisks
737 denote (a) keystone taxa in the core community of one or more sites, or (b) core taxa that were
738 also keystone. Note the differing colour scales. Labels provide the lowest taxonomic level
739 identified for the ASV.
740
741 **Figure 4** Barplot of clusters of orthologous genes (COGs) on cane toad skin. Each vertical bar is a
742 single toad sample, grouped by site.
743
744 **Figure 5** Cane toad skin bacterial functional communities from five geographic regions with
745 increasing functional grouping from (a) KEGG orthology to (b) KEGG modules to (c) COGs. One
746 toad site per region (colour-coded) was examined for functional differences. Points are average
747 values per site, with rays ending at individual bacterial community values.
748
749
750
751
752

Figure 1

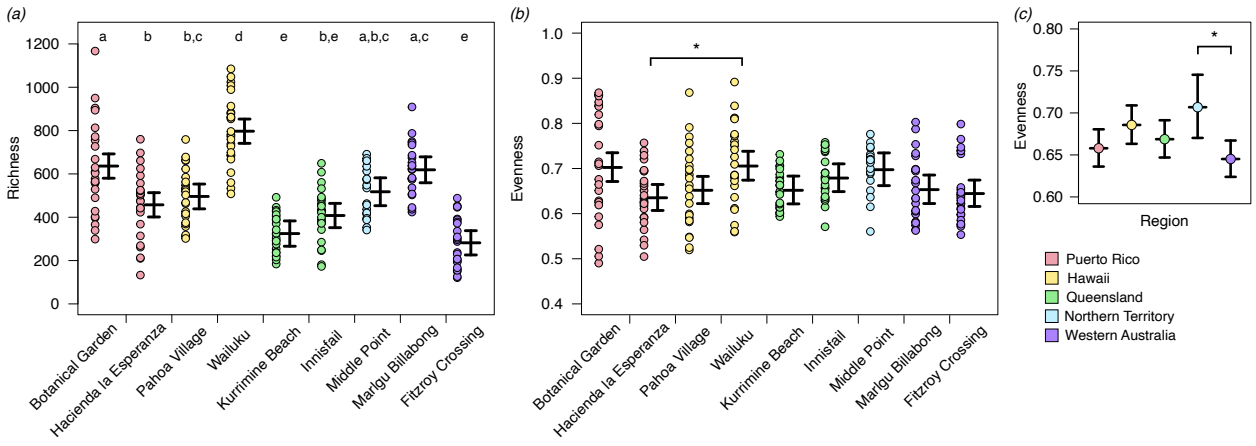

Figure 2

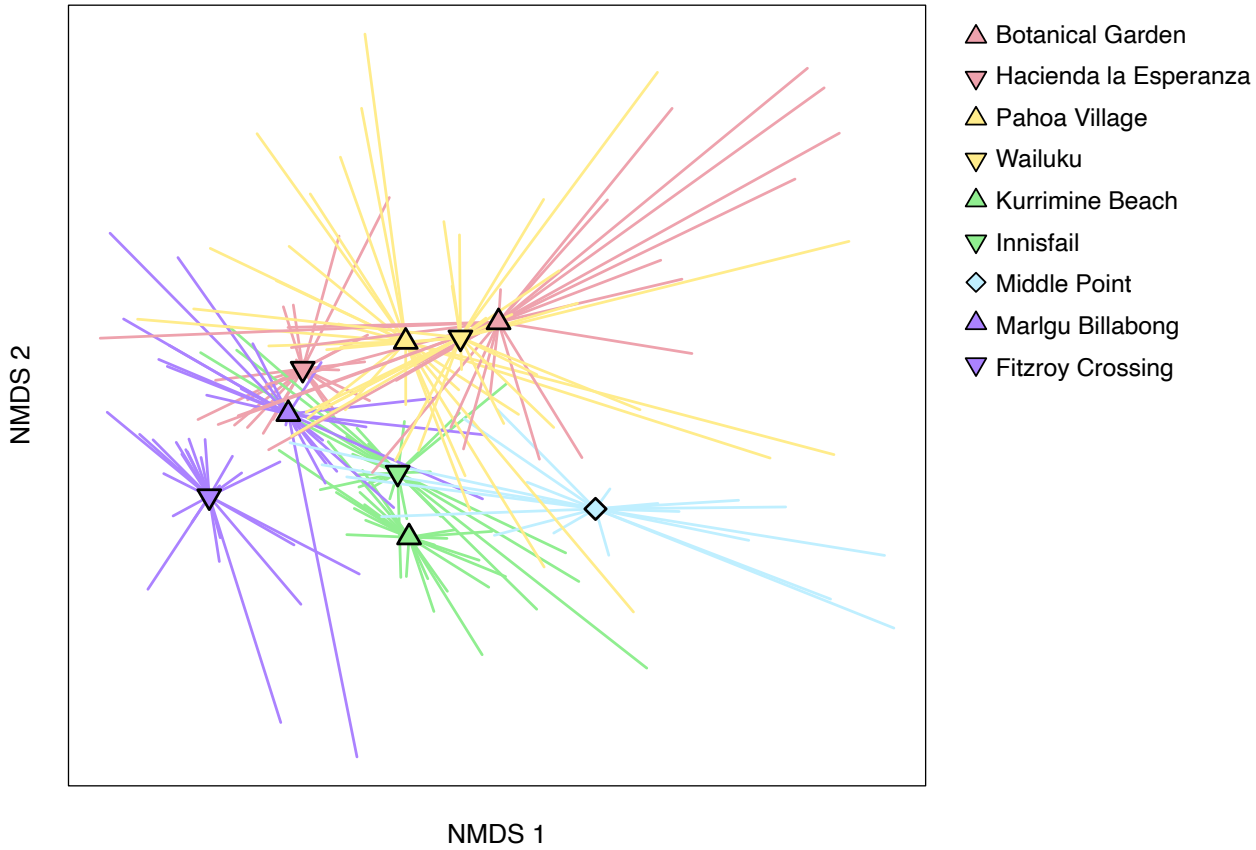

Figure 3

(a) Keystone ASVs

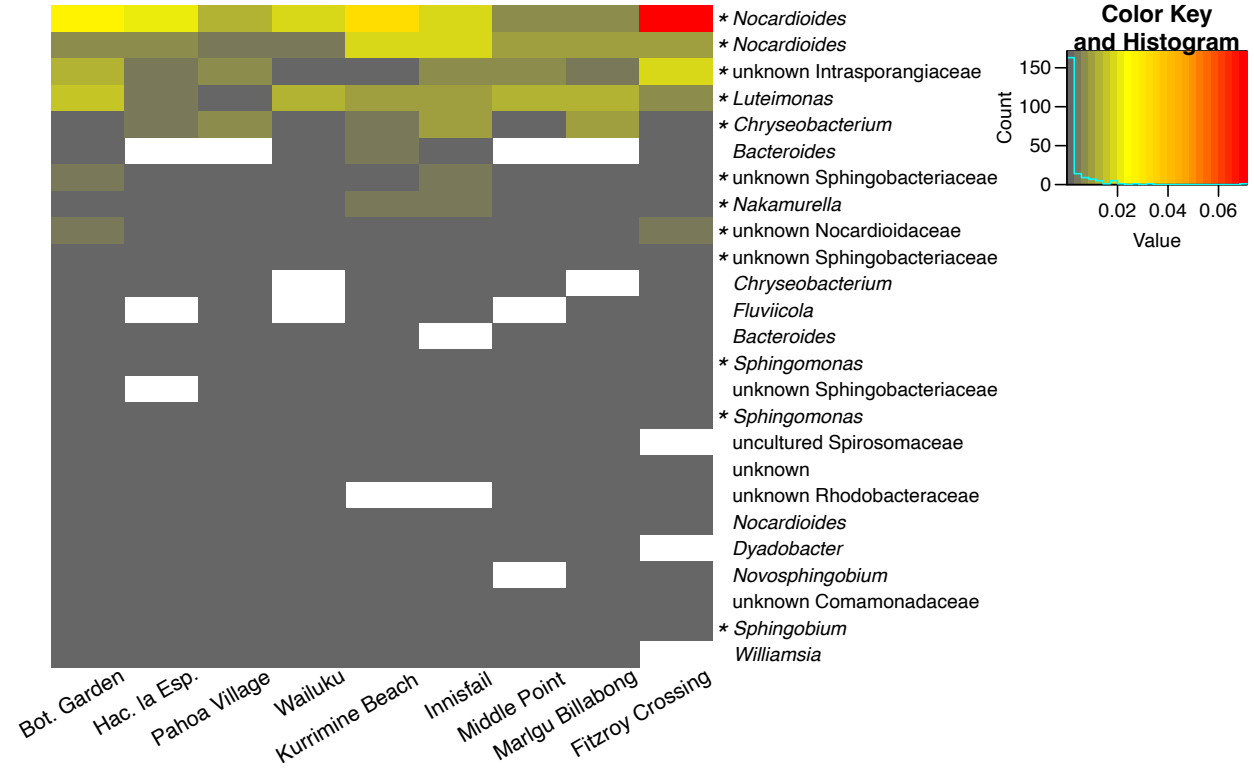

(b) Core ASVs

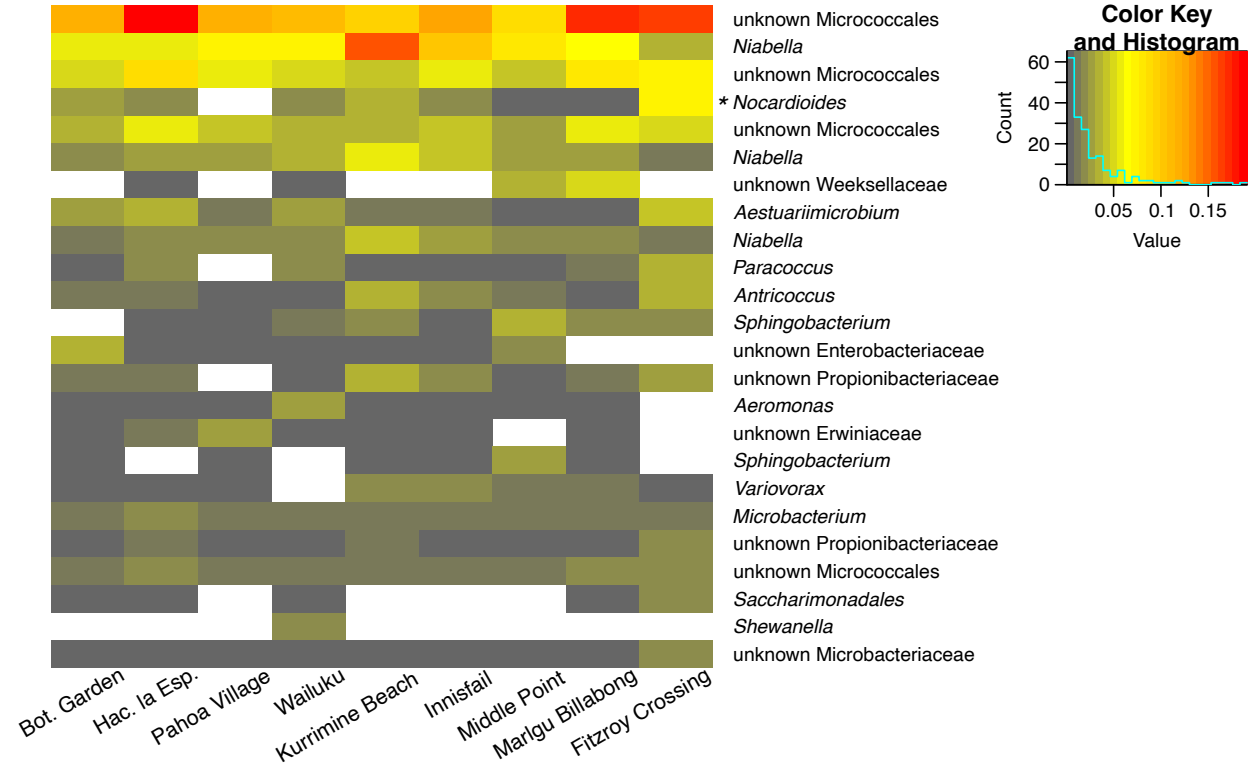

762 **Figure 4**

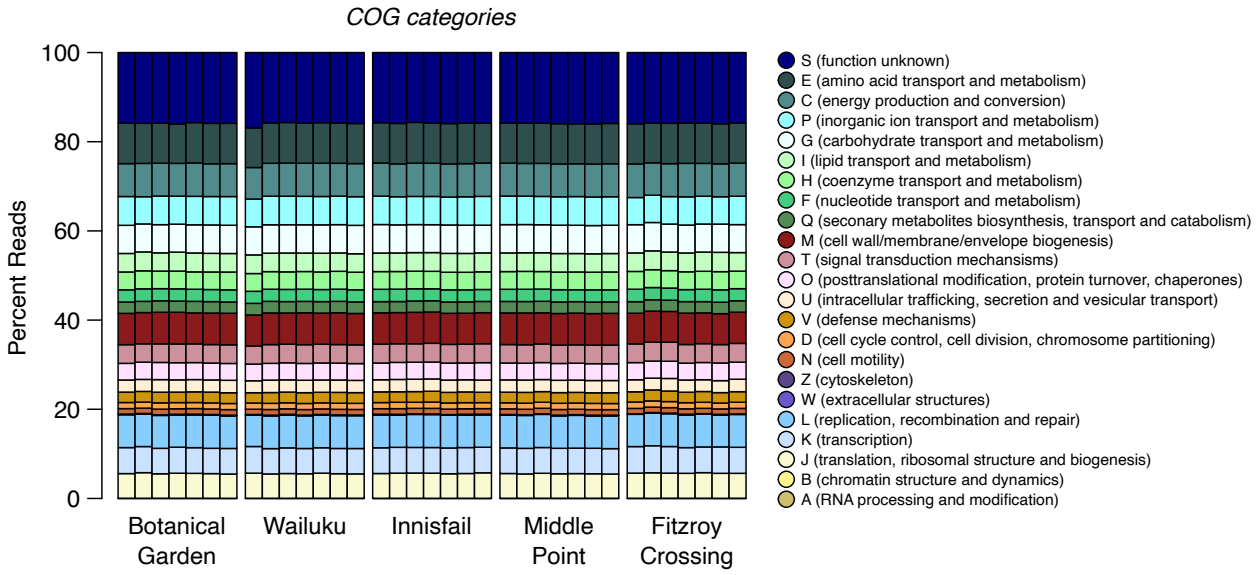

763

764

765 **Figure 5**

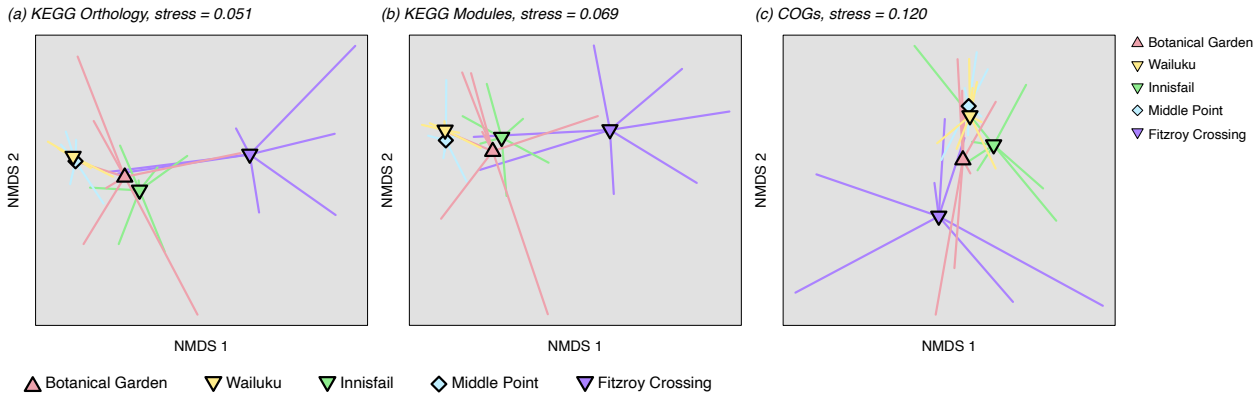

766

Supplemental Materials

Structural and functional skin microbiota on cane toads across 16,000 km of invaded range

Chava L. Weitzman*[1], chava.weitzman2@cdu.edu.au, ORCId - 0000-0002-6103-1885

Kimberley Day[1], k.day@aims.gov.au

Gregory P. Brown[2], greg.brown@mq.edu.au, ORCId - 0000-0002-2924-9040

Karen Gibb[1], karen.gibb@cdu.edu.au, ORCId - 0000-0003-2987-883X

Keith Christian[1], keith.christian@cdu.edu.au, ORCId - 0000-0001-6135-1670

[1] Research Institute for the Environment and Livelihoods, Charles Darwin University, Darwin, NT, 0909, Australia

[2] Department of Biological Sciences, Macquarie University, New South Wales, 2109, Australia

*Corresponding author: chava.weitzman2@cdu.edu.au

Summary

To complement the alpha diversity results, Figure S1 provides the relationship between ASV evenness and toad size (SVL).

In addition to ASV diversity, each diversity metric was evaluated on the level of bacterial genus. Fewer community differences on the genus level would suggest that the maintenance of community function is a result of, at least in part, microdiversity within genera (García-García et al. 2019). Results of analyses of diversity based on bacterial genera are available in Figure S2 and Tables S1 and S2. Figure S3 provides information on keystone and core genera. Table S3 provides statistical results of Mantel tests comparing beta diversity based on bacterial genera and the three levels of functional diversity.

Because many ASVs and genera were found to be in the core communities among the sampling sites, we provide UpSet plots of core ASVs (Figure S4) and genera (Figure S5) to visualise the frequency of overlapping taxa among the sites.

Lastly, we used these data, alongside a dataset of wild cane toad samples collected over a period of two years (Weitzman et al. 2025), to detect taxa persistent over space and time. Further information on these taxa and their relative abundance in the communities is available in Tables S4–S7.

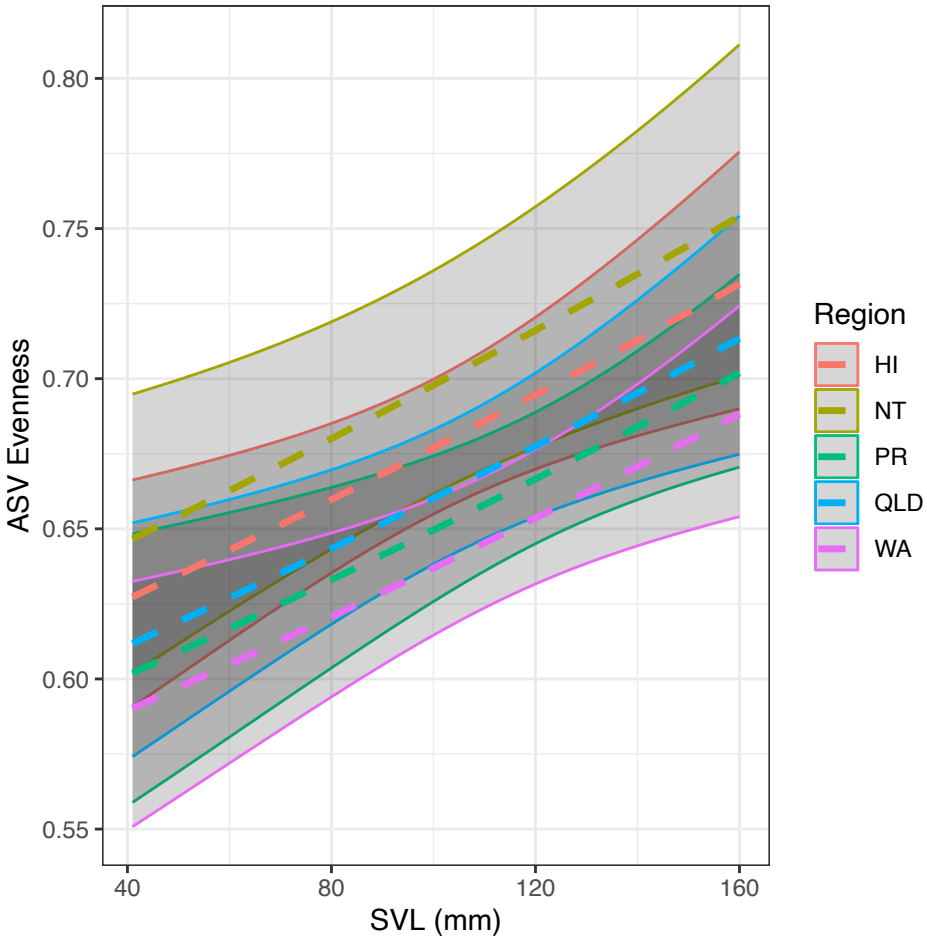

Figure S1 Evenness increases with toad size. Predicted values are colour-coded by toad region based on the linear model (log(evenness) ~ Region + SVL).

Table S1 Top five models identifying drivers of alpha diversity of bacterial genera on cane toad skin from linear models. *P*-value is provided for each predictor. **Bold** denotes best model for each metric based on ΔAICc < 2.

Models	AICc	ΔAICc	Model *P*	Site	Region	SVL	Mass	Sex
Genus, Richness								
Site	**2191.59**	**0**	**< 0.0001**	**< 0.0001; $F_{(8,204)}$ = 33.68**				
Region + SVL + Sex	2320.13	128.5	< 0.0001		< 0.0001; $F_{(4,206)}$ = 10.01	0.006; $F_{(1,206)}$ = 7.82		0.04; $F_{(1,206)}$ = 4.12
Region + SVL	2322.19	130.6	< 0.0001		< 0.0001; $F_{(4,207)}$ = 10.27	0.005; $F_{(1,207)}$ = 8.02		
Region + Sex	2325.90	134.3	< 0.0001		< 0.0001; $F_{(4,207)}$ = 8.54			0.04; $F_{(1,207)}$ = 4.31
Region + Mass + Sex	2327.06	135.5	< 0.0001		< 0.0001; $F_{(4,206)}$ = 8.74		0.3; $F_{(1,206)}$ = 0.97	0.03; $F_{(1,206)}$ = 4.58
Genus, Evenness								
Site	**-421.15**	**0**	**< 0.0001**	**< 0.0001; $F_{(8,204)}$ = 4.76**				
Region + SVL + Sex	-412.63	8.5	0.0008		0.009; $F_{(4,206)}$ = 3.50	0.0005; $F_{(1,206)}$ = 12.56		0.06; $F_{(1,206)}$ = 3.67
Region + SVL	-411.03	10.1	0.002		0.02; $F_{(4,207)}$ = 3.02	0.0004; $F_{(1,207)}$ = 12.79		
SVL	-407.39	13.8	0.006			0.006; $F_{(1,211)}$ = 7.82		
SVL + Sex	-407.13	14.0	0.009			0.01; $F_{(1,210)}$ = 6.77		0.2; $F_{(1,210)}$ = 1.80

Table S2 Beta diversity of bacterial genera on cane toad skin is strongly explained by host site. Top five permutational MANOVA models and R^2 for relevant predictors. **Bold** denotes best model based on ΔAICc < 2.

Models	AICc	ΔAICc	Site	Region	SVL	Mass	Sex
Site	**-509.31**	**0.0**	**0.383**				
Region + SVL + Sex	-474.69	34.6		0.204	0.025		0.014
Region + Mass + Sex	-473.32	36.0		0.203		0.020	0.014
Region + SVL	-472.93	36.4		0.218	0.025		
Region + Mass	-471.40	37.9		0.217		0.020	

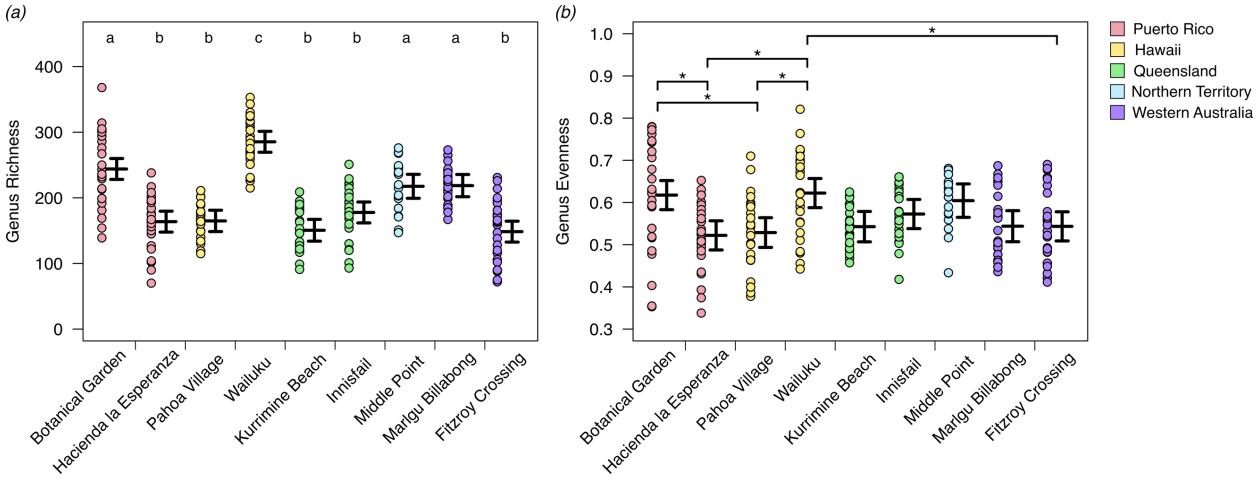

Figure S2 Richness (a) and evenness (b,c) of bacterial genera on cane toad skin by host site. Points provide raw data and are colour-coded by region for context. Bars are estimated marginal means and 95% confidence intervals. Differing letters above values in (a) and asterisks in (b) denote toad sites with significantly different diversity in pairwise tests.

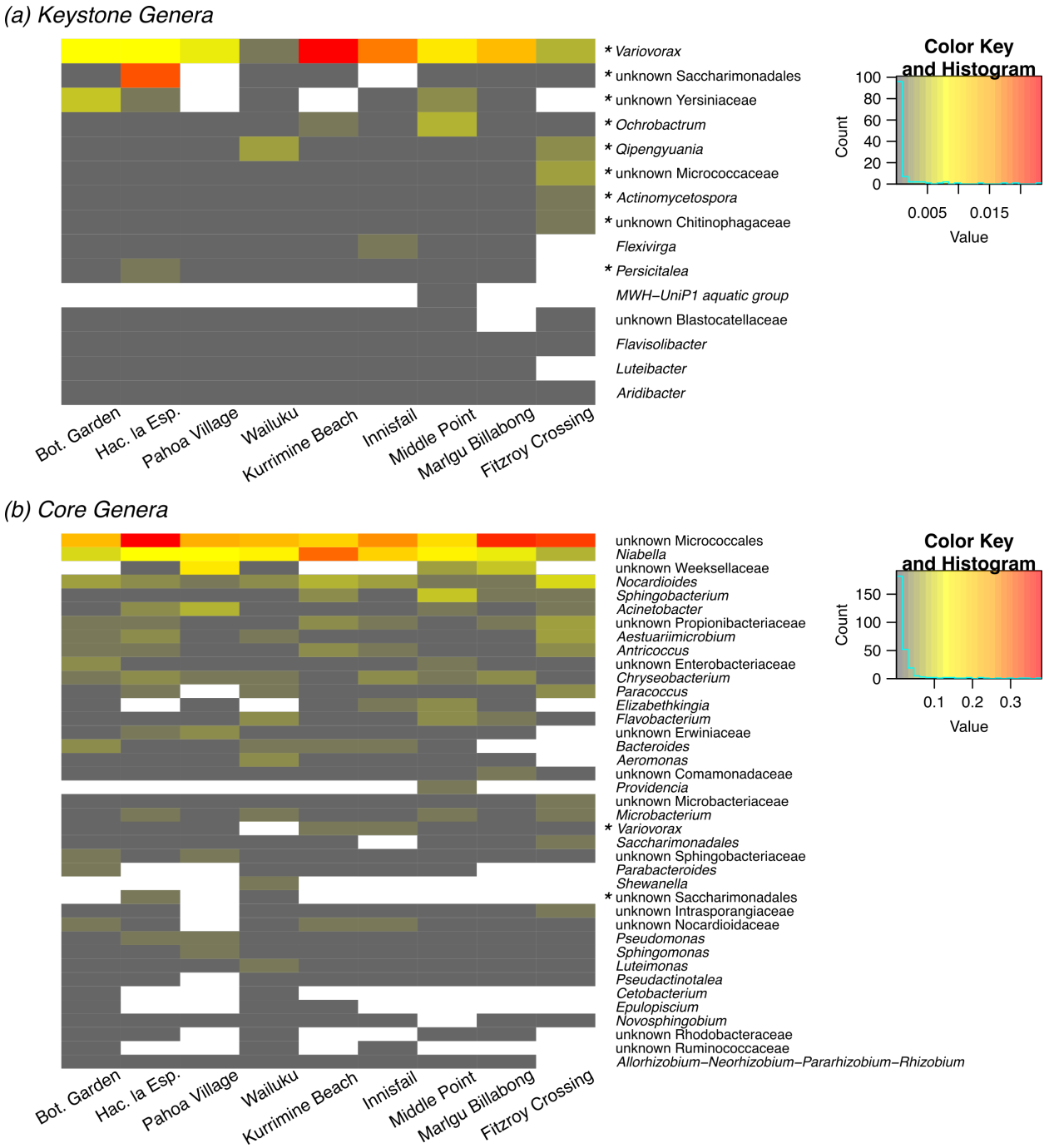

Figure S3 Keystone and core bacterial genera in cane toad skin communities. Both were identified with the full dataset, with n = 25 toad samples per site. (a) Keystone bacterial genera identified by eigenvectors in a SPRING network constructed from the 300 genera with the highest frequencies. Colours denote the average relative abundance in the site. White indicates the genus was absent from that toad site. (b) Core genera (or lowest taxonomic level identified; >90% prevalence) subset to those representing on average > 1% relative abundance in a relevant community. Colours denote average relative abundances per toad site that the taxon was present in the core community. White indicates the taxon was not core in the site (i.e., it may have been present, but not in the site's core community). Asterisks denote (a) keystone taxa in the core community of one or more sites, or (b) core taxa that were also keystone. Note the differing colour scales. None of the 19

genera that were core in all nine sites was also a keystone genus. Of the nine keystone genera that were also core, most were only core/prevalent in one to three sites, except for *Variovorax*.

Table S3 Results of Mantel tests comparing community structure based on bacterial genera and three levels of community function. **Bold** denotes significant correlations.

Comparison	r	Significance (without strata)	Significance (with strata)
Genera v KEGG orthology	**0.277**	**0.005**	**0.004**
Genera v KEGG modules	**0.257**	**0.006**	**0.011**
Genera v COGs	0.057	0.06	0.2

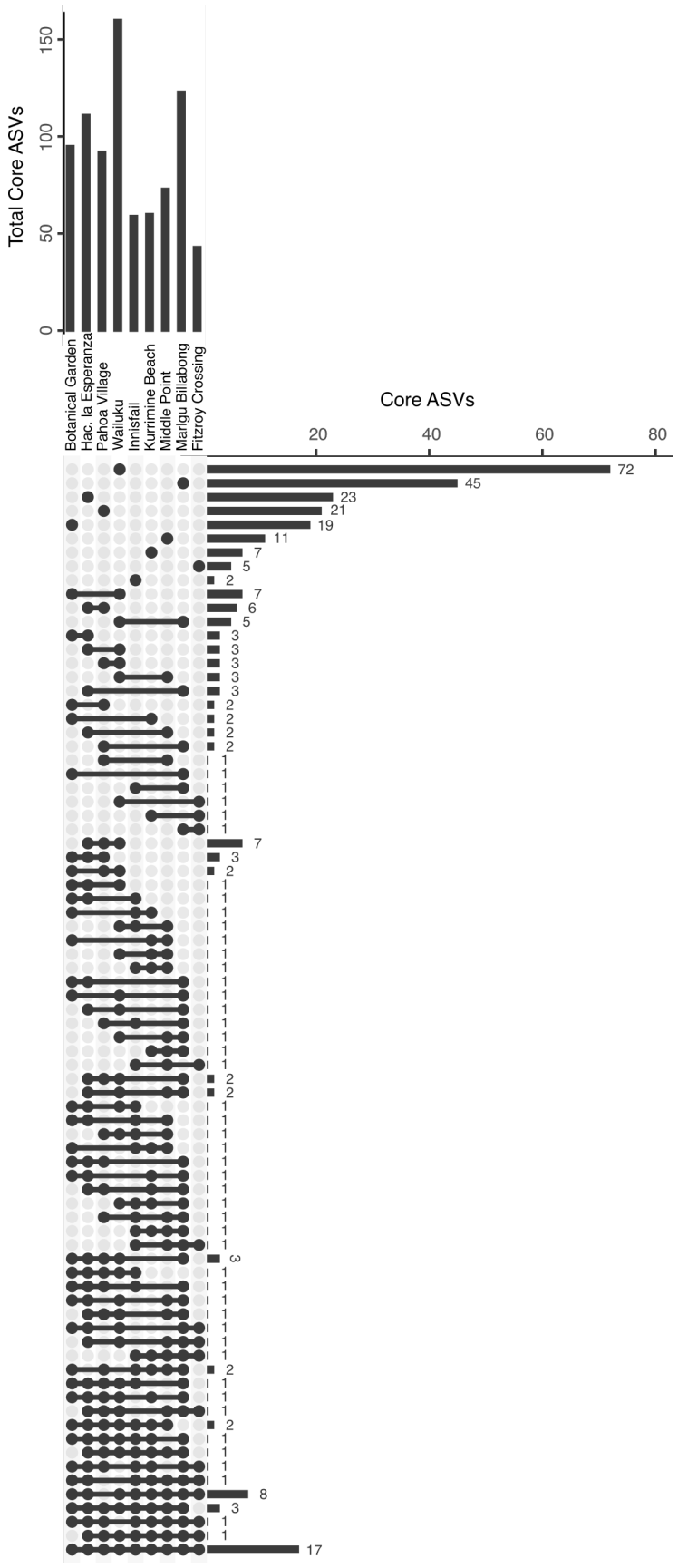

Figure S4 UpSet plot of core ASVs in cane toad skin bacterial communities in nine sampled sites. Core taxa were identified as those present in 90% of samples per site (N = 25 toads sampled per site). Vertical bars indicate the total number of core ASVs for the communities at each site. Horizontal bars indicate the number of core taxa unique to a site (when one site is highlighted) or shared in the core communities of multiple sites (identified by highlighted site indicators).

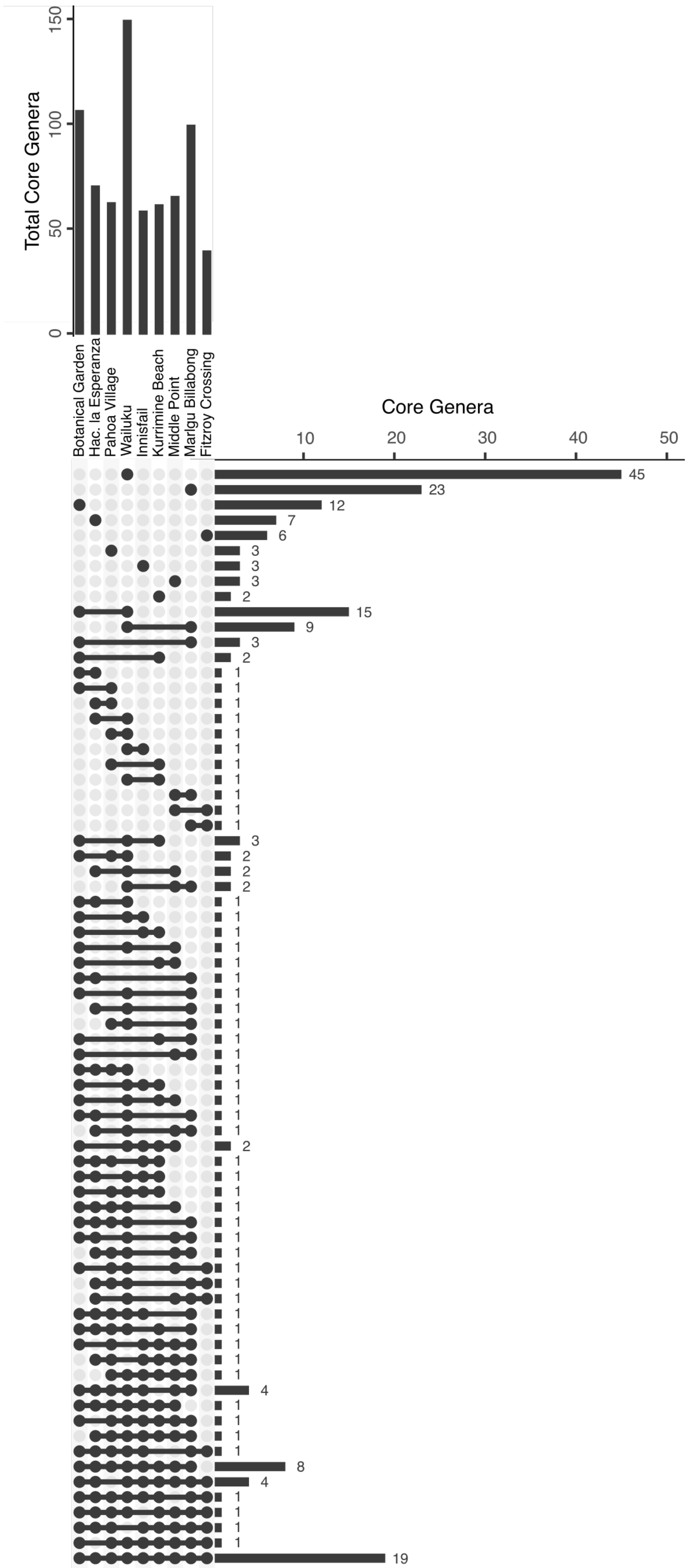

Figure S5 UpSet plot of core genera (or lowest taxonomic level) in cane toad skin bacterial communities in nine sampled sites. Core taxa were identified as those present in 90% of samples per site (N = 25 toads sampled per site). Horizontal bars indicate the number of core taxa unique to a site (when one site is highlighted) or shared in the core communities of multiple sites (identified by highlighted site indicators).

Table S4 Bacterial genera present in 90% of the samples in the present, spatial study of cane toads, and also present in 90% of samples collected from wild toads from Middle Point, Australia during a temporal study (N = 82 toads; Weitzman et al. 2025). Cores for each are based off of unrarefied data. Genera are in alphabetical order.

Bacterial genus
Acinetobacter
Aeromonas
Antricoccus
Bacillus
Bacteroides
Chryseobacterium
Flavobacterium
Luteimonas
Methylobacterium-Methylorubrum
Niabella
Nocardioides
Paracoccus
Pseudactinotalea
Pseudomonas
Sphingobacterium
Sphingomonas

Table S5 Mean proportions of reads per cane toad sample assigned to core genera. Core genera are those present in 90% of samples from the present spatial experiment and also present in 90% of wild samples from a temporal experiment (Weitzman et al. 2025). Mean proportions presented for all of the samples in each experiment, as well as for each site (spatial experiment) or sampling time point (temporal experiment). Samples from the temporal experiment were collected from Middle Point, NT, Australia. Warmer colours indicate larger mean proportions, from yellow (20%s) to red-orange (50%s).

	Mean Proportion Core ± SD	
Spatial	*0.373 ±0.1183 (all)*	
San Juan Botanical Garden	0.306 ± 0.0919	
Hacienda la Esperanza	0.335 ± 0.0633	
Pahoa	0.326 ± 0.1007	
Wailuku	0.380 ± 0.0889	
Kurrimine Beach	0.543 ± 0.1009	
Innisfail	0.417 ± 0.1067	
Middle Point	0.421 ± 0.0797	
Marlgu Billabong	0.286 ± 0.1051	
Fitzroy Crossing	0.341 ± 0.0950	
Temporal	*0.469 ±0.1309 (all)*	
10-May-2021	0.491 ± 0.1214	
20-Jul-2021	0.398 ± 0.0942	
23-Feb-2022	0.462 ± 0.1440	
6-Jun-2022	0.509 ± 0.1213	
9-Feb-2023	0.425 ± 0.1425	
23-May-2023	0.489 ± 0.1323	

Table S6 Bacterial families present in 90% of the samples in the present, spatial study of cane toads, and also present in 90% of samples collected from wild toads from Middle Point, Australia during a temporal study (N = 82 toads; Weitzman et al. 2025). Cores for each are based off of unrarefied data. Families are in alphabetical order.

Bacterial family
Aeromonadaceae
Bacillaceae
Bacteroidaceae
Beijerinckiaceae
Cellulomonadaceae
Chitinophagaceae
Comamonadaceae
Enterobacteriaceae
Erysipelotrichaceae
Flavobacteriaceae
Geodermatophilaceae
Intrasporangiaceae

Bacterial family (cont.)
Lachnospiraceae
Microbacteriaceae
Moraxellaceae
Nocardioidaceae
Pseudomonadaceae
Rhizobiaceae
Rhodobacteraceae
Sphingobacteriaceae
Sphingomonadaceae
Spirosomaceae
Weeksellaceae
Xanthomonadaceae

Table S7 Mean proportions of reads per cane toad sample assigned to core families. Core families are those present in 90% of samples from the present spatial experiment and also present in 90% of wild samples from a temporal experiment (Weitzman et al. 2025). Mean proportions presented for all of the samples in each experiment, as well as for each site (spatial experiment) or sampling time point (temporal experiment). Samples from the temporal experiment were collected from Middle Point, NT, Australia. Warmer colours indicate larger mean proportions, from orange (40%s) to red (70%s).

	Mean Proportion Core ± SD	
Spatial	*0.576 ±0.1308 (all)*	
San Juan Botanical Garden	0.515 ± 0.0976	
Hacienda la Esperanza	0.472 ± 0.0880	
Pahoa	0.635 ± 0.1399	
Wailuku	0.551 ± 0.0818	
Kurrimine Beach	0.690 ± 0.0992	
Innisfail	0.608 ± 0.1202	
Middle Point	0.687 ± 0.1062	
Marlgu Billabong	0.550 ± 0.1069	
Fitzroy Crossing	0.477 ± 0.1077	
Temporal	*0.689 ±0.1342 (all)*	
10-May-2021	0.668 ± 0.1351	
20-Jul-2021	0.549 ± 0.1233	
23-Feb-2022	0.734 ± 0.1332	
6-Jun-2022	0.754 ± 0.0937	
9-Feb-2023	0.690 ± 0.1254	
23-May-2023	0.665 ± 0.1402	

Supplemental References

García-García, N., J. Tamames, A. M. Linz, C. Pedrós-Alió, and F. Puente-Sánchez. 2019. Microdiversity ensures the maintenance of functional microbial communities under changing environmental conditions. The ISME Journal 13:2969–2983.

Weitzman, C. L., K. Day, G. P. Brown, K. Gibb, and K. Christian. 2025. Differential temporal shifts in skin bacteria on wild and captive toads. Microbial Ecology 88:35.